Antiviral Research 88 (2010) 281–286

Contents lists available at ScienceDirect

Antiviral Research

journal homepage: www.elsevier.com/locate/antiviral

Dynamic escape of pre-existing raltegravir-resistant HIV-1 from raltegravir selection pressure

Francisco M. Codoñer[a], Christian Pou[a], Alexander Thielen[c], Federico García[d], Rafael Delgado[e], David Dalmau[f], José Ramon Santos[b], Maria José Buzón[a], Javier Martínez-Picado[a,g], Miguel Álvarez-Tejado[h], Bonaventura Clotet[a,b], Lidia Ruiz[a], Roger Paredes[a,b,*]

[a] *IrsiCaixa Retrovirology Laboratory-HIVACAT, Hospital Universitari Germans Trias i Pujol, Badalona, Spain*
[b] *Lluita Contra la SIDA Foundation, Hospital Universitari Germans Trias i Pujol, Badalona, Spain*
[c] *Max Planck Institute für Informatik, Saarbücken, Germany*
[d] *Hospital Universitario San Cecilio, Granada, Spain*
[e] *Hospital 12 de Octubre, Madrid, Spain*
[f] *Hospital Universitari Mútua de Terrassa, Terrassa, Spain*
[g] *Institució Catalana de Recerca i Estudis Avançats (ICREA), Barcelona, Spain*
[h] *Roche Diagnostics SL, Sant Cugat del Vallès, Spain*

ARTICLE INFO

Article history:
Received 13 August 2010
Received in revised form
17 September 2010
Accepted 21 September 2010

Keywords:
HIV-1
Antiretroviral resistance
Deep sequencing
Raltegravir
Evolution

ABSTRACT

Using quantitative deep HIV-1 sequencing in a subject who developed virological failure to deep salvage therapy with raltegravir, we found that most Q148R and N155H mutants detected at the time of virological failure originated from pre-existing minority Q148R and N155H variants through independent evolutionary clusters. Double 148R + N155H mutants were also detected in 1.7% of viruses at virological failure in association with E138K and/or G163R. Our findings illustrate the ability of HIV-1 to escape from suboptimal antiretroviral drug pressure through selection of pre-existing drug-resistant mutants, underscoring the importance of using fully active antiretroviral regimens to treat all HIV-1-infected subjects.

1. Introduction

Integrase strand transfer inhibitors are a new family of antiretrovirals that reached HIV clinics in 2007 (McColl and Chen, 2010; Steigbigel et al., 2008). Resistance to raltegravir, the first integrase inhibitor available for HIV treatment, evolves through three seemingly exclusive pathways (Fransen et al., 2009) characterized by a signature mutation in the integrase catalytic centre (Y143R/C, Q148R/H/K or N155H) plus several accessory mutations that increase resistance or improve viral replication (Cooper et al., 2008; Paredes and Clotet, 2010). Clonal analyses suggested that Q148R/H/K and N155H mutations did not coexist in individual genomes, which is consistent with the low replication capacity of double Q148R/H/K + N155H mutants *in vitro* (Fransen et al., 2009; McColl and Chen, 2010). The fitness impact of raltegravir resistance mutations, however, may be modulated *in vivo* by accessory mutations in integrase, as well as by epistatic effects of other HIV-1 genes (Buzon et al., 2010).

2. Clinical case

We report the case of a 42 year-old male diagnosed with HIV in 1988 (Fig. 1) with history of alcoholism and illicit drug use until 1993. He was treated for pulmonary tuberculosis and *Pneumocystiis jirovecii* pneumonia in 1993 and 2004, respectively. Although he had good adherence to antiretrovirals in the recent years, he never achieved HIV-1 RNA suppression <50 copies/mL and his CD4+ T cell counts remained extremely low (the nadir and zenith CD4+ counts were, respectively, 1 and 169 cells/mm^3). After receiving 13 different antiretrovirals during 15 years, he began salvage therapy with tenofovir disoproxil fumarate (245 mg QD), raltegravir (200 mg BID), darunavir (600 mg BID) and ritonavir (100 mg BID) on July 2007. HIV-1 RNA levels decreased 2 $\log_{10}$ four weeks after

* Corresponding author at: HIV Unit & Institut de Recerca de la SIDA – IrsiCaixa, Hospital Universitari Germans Trias i Pujol, Universitat Autònoma de Barcelona, Crta. de Canyet s/n, Planta 2a, 08916 Badalona, Catalonia, Spain.
Tel.: +34 93 465 6374x162; fax: +34 93 465 3968.
E-mail address: rparedes@irsicaixa.es (R. Paredes).

0166-3542/$ – see front matter © 2010 Elsevier B.V. All rights reserved.
doi:10.1016/j.antiviral.2010.09.016

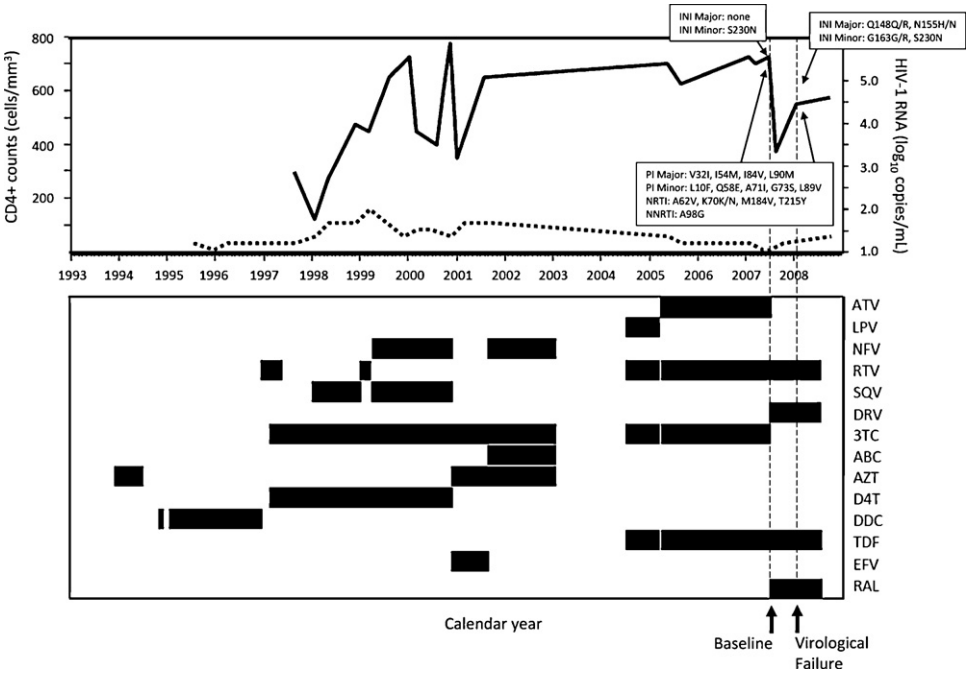

Fig. 1. Antiretroviral treatment history and virological and immunological evolution. The continuous line in the upper graph represents HIV-1 RNA levels in copies/mL transformed in a logarithmic scale; the dashed line in the upper graph represents CD4+ T-cell counts (CD4 counts) in cells/mm^3. Horizontal bars in the lower graph represent the time period during which a given antiretroviral drug was prescribed. Vertical dashed lines represent the timepoints when population and quantitative deep sequencing was performed; i.e., baseline and virological failure. Boxes include resistance mutations detected by population sequencing at baseline and virological failure. PI: protease inhibitor; NRTI: nucleoside reverse transcriptase inhibitor; NNRTI: non-nucleoside reverse transcriptase inhibitor; IN: integrase; ATV: atazanavir; LPV: lopinavir; NFV: nelfinavir; RTV: ritonavir; SQV: saquinavir; DRV: darunavir; 3TC: lamivudine; ABC: abacavir; AZT: zidovudine; D4T: stavudine; DDC: zalcitabine; TDF: tenofovir diprivoxil fumarate; EFV: efavirenz; RAL: raltegravir; None: antiretroviral treatment interruption. Graph developed with and adapted from the ART-AiDE (Antiretroviral Therapy – Acquisition & Display Engine) Program, Stanford HIV Drug Resistance Database.

therapy initiation, but rebounded 1 $\log_{10}$ twenty weeks later. A few weeks after virological failure, the patient was admitted to the intensive care unit and died of acute respiratory distress.

3. Methods

3.1. HIV-1 population and quantitative deep sequencing

HIV-1 RNA was extracted from 1 mL of plasma 3 weeks before initiation of salvage antiretroviral therapy (baseline) and at virological failure (VF), 24 weeks after treatment initiation. Plasma was centrifuged at 35,000 rpm (9000 × *g*) during 90 min at 4 °C. Viral pellets were resuspended and viral RNA was extracted (QIAamp UltraSens Virus Kit™, QIAGEN, Valencia, CA). Three One-Step RT-PCRs (SuperScript® III One-Step RT-PCR System with Platinum® Taq High Fidelity, Invitrogen, Carlsbad, CA) were performed in parallel per each sample. Primers used were 1571-L23 (HXB2: 1417 → 1440) 5′-ATT TCT CCT ACT GGG ATA GGT GG-3′ and 5464-L27 (HXB2: 5464 → 5438) 5′-CCT TGT TAT GTC CTG CTT GAT ATT CAC-3′. Cycling conditions were: 30 min at 52 °C, 2 min at 94 °C; 30 s at 94 °C, 30 s at 56 °C, 4 min at 68 °C, for 30 cycles; followed by 5 min at 68 °C. Triplicate RT-PCR products were pooled, column-purified (QIAquick PCR Purification Kit, QIAGEN, Valencia, CA) and used for both viral population and quantitative deep HIV-1 sequencing (QDS).

3.1.1. Viral population genotyping

For population sequencing, triplicate nested PCRs were performed in parallel (Platinum® Taq DNA Polymerase High Fidelity, Invitrogen, Carlsbad, CA) with primers 2084-U26 (HXB2: 2084 → 2109) 5′-ATT TTT TAG GGA AGA TCT GGC CTT CC-3′ and 5456-L26 (HXB2: 5456 → 5431) 5′-TGT CCT GCT TGA TAT TCA CAC CTA GG-3′. Cycling conditions were: 2 min at 94 °C; 30 s at 94 °C, 30 s at 56 °C, 4 min at 68 °C, for 30 cycles; followed by 5 min at 68 °C. Again, nested PCR products were pooled and column-purified (QIAquick PCR Purification Kit, QIAGEN, Valencia, CA). Protease, reverse transcriptase and integrase genes were sequenced in-house (BigDye v3.1, Applied Biosystems, Foster City, CA, USA) and resolved by capillary electrophoresis (ABI 7000, Foster City, CA, USA). Genotypes were interpreted automatically with the HIVdb program implemented in the Stanford drug resistance database (Liu and Shafer, 2006; Rhee et al., 2003).

3.1.2. Quantitative deep sequencing

Pooled purified RT-PCR products were used as template to generate two overlapping amplicons. Excluding primer sites, amplicon 1 encompassed the integrase codons 91 to 178 (HXB2: 4499–4763), whereas amplicon 2 included the integrase codons 132 to 224 (HXB2: 4621–4900). The overlapping region between the two amplicons thus encompassed codons 132–178 in the Integrase catalytic center (HXB2: 4621–4763). Each amplicon was generated in triplicate during 30 cycles of PCR amplification (Platinum® Taq DNA Polymerase High Fidelity, Invitrogen, Carlsbad, CA). Primers for amplicon 1 were Beta-F (HXB2: 4481 → 4499) 5′- AGA AGC AGA AGT TAT TCC A -3′ and Beta R (HXB2 4763 → 4780) 5′-TTG TGG ATG AAT ACT GCC-3′; primers for amplicon 2 were Gamma-F (HXB2: 4606 → 4621) 5′- TTA AGG CCG CCT GTT G -3′ and Gamma R (HXB2: 4900 → 4917) 5′-TGT CCC TGT AAT AAA CCC-3′. In addition, primers contained 454 sequencing adapters A or B and 8-nucleotide sample identifier tags in the 5′-end. Triplicate PCR products were pooled and purified (QIAquick PCR Purification Kit, QIAGEN, Valencia, CA). Quantitative Deep Sequencing was performed at 454 Life Sciences, Branford, CT, USA.

Raw output sequences were filtered to ensure high quality (Table 1). The overlapping region between the two amplicons (integrase codons 132–178) was extracted. Sequences resulting

Table 1
Filtering of sequences obtained by quantitative deep sequencing.

		HXB2 position range[a]	Integrase codon range[a]	Reads	Sequences filtered out (homology < 90%)	Sequences left	Unique sequences
Baseline	Amplicon 1	4499–4763	91–178	1951	312	1639	N/A
	Amplicon 2	4621–4900	132–224	1852	100	1752	N/A
	Overlap[b]	4621–4763	132–178	3803	412	3391	222
Virological failure	Amplicon 1	4499–4763	91–178	2506	456	2050	N/A
	Amplicon 2	4621–4900	132–224	1409	75	1334	N/A
	Overlap[b]	4621–4763	132–178	3915	531	3384	311

[a] Excluding primer sites.
[b] Overlapping regions of the 2 amplicons; N/A, not applicable.

from extraction were selected if they had more than 90% similarity with the consensus sequence of the run for that subject and region. Sequencing errors in homopolymeric regions were manually inspected and corrected. Sequences that included a stop codon were removed. The sequence coverage was calculated for each aminoacid position. Unique sequences were identified and the percentage of specific mutations in the 143, 148 or 155 positions as well as the percentage of double and triple mutants was calculated only in those sequences surpassing all the abovementioned quality filters.

An in-house analysis of 992 pNL43 clonal sequences obtained by quantitative deep sequencing under the same PCR conditions used to generate patient samples showed a mean (SD) nucleotide mismatch rate of 0.07% (0.13%), similar to previous reports (Varghese et al., 2009). The mean (SD) error rate for any aminoacid mismatch was 0.14% (0.19%), but the mean (SD) error rate for actual drug resistance mutations was 0.03% (0.07%). The 99th percentile of mismatches would establish the threshold for nucleotide errors in 0.61% and the limit for identifying true drug resistance mutations in 0.20%.

3.2. Phylogenetic analysis

Unique overlapping sequences obtained with QDS were used to build a protein Multiple Sequence Alignment (MSA) using Musclev3.7 (Edgar, 2004). Sequence indeterminations were substituted for gaps and were subsequently removed. In addition, a DNA MSA was built concatenating triplets of bases according to the protein MSA. The protein alignment was used to identify the best fit molecular evolutionary model using PROTTEST v2.2 (Abascal et al., 2005). The evolutionary model obtained was used to build a maximum likelihood phylogenetic tree with PHYMLv3.0 (Guindon and Gascuel, 2003). MEGA v4.1 (Kumar et al., 2004) was used to build the tree topology based on a Neighbor-Joining approach, using a pairwise deletion, with the best evolutionary model found by PROTTEST and implemented in MEGA as a distance model. A Simodaira Hasegawa test was used to assess the most likely tree topology to explain the sequence evolution (Shimodaira and Hasegawa, 1999).

To further investigate the origin of Q148R and N155H mutants detected at the time of VF using an independent phylogenetic

Table 2
Linkage analysis of major and accessory integrase inhibitor resistance mutations at virological failure by quantitative deep sequencing.

Major mutation	Accessory mutations in integrase codons					#Clones	% Relative to clones with the major mutation	% Relative to total clones at virological failure
	138	140	151	163	Other[a]			
Consensus B	E	G	V	G	N/A			
Q148R	K					895	53.56	26.45
		S				357	21.36	10.55
		S		R		143	8.56	4.23
						109	6.52	3.22
	K			R		93	5.57	2.75
					X	74	4.43	2.19
N155H				R		1353	85.47	39.98
						111	7.01	3.28
	K			R		41	2.59	1.21
					X	78	4.93	2.31
Q148R + N155H	K			R		31	53.43	0.92
				R		9	15.53	0.27
		S		R		9	15.53	0.27
	K					7	12.07	0.21
						1	1.73	0.03
		S				1	1.73	0.03
Y143H + Q148R	K					1	33.33	0.03
	K					1	33.33	0.03
		S		R		1	33.33	0.03
Y143C + N155H				R		3	100	0.09
Y143H + N155H				R		8	100	0.24

N/A, not applicable.
[a] Only clones representing > 1% of the total sequences obtained by quantitative deep sequencing at virological failure are shown for single Q148R and N155H major mutants; all clones are shown for dual major mutants. "Other" includes the sum of all clones being detected in less than 1% of the total sequences at virological failure that show mutation combinations different from the ones presented in the table; other combinations are represented by "X".

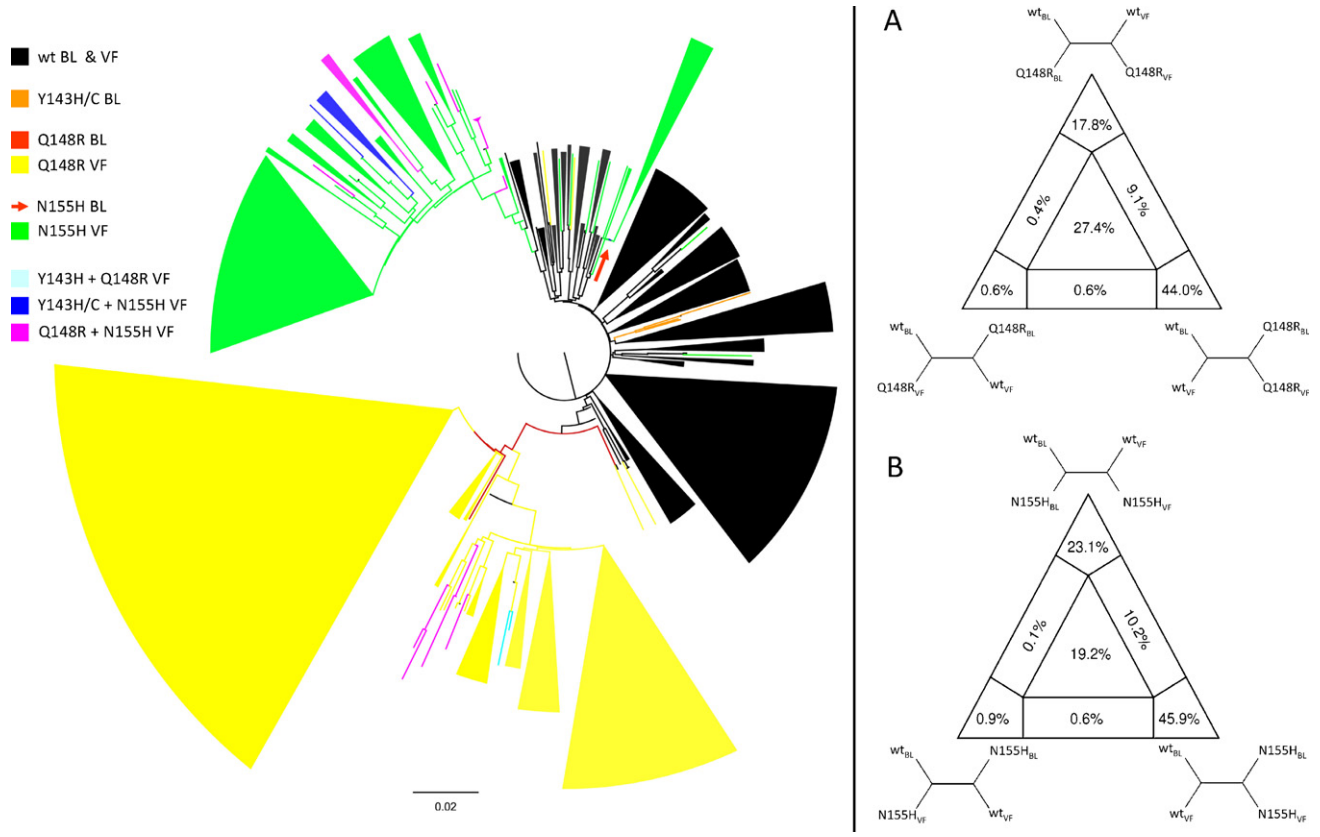

Fig. 2. Origin of viruses escaping raltegravir pressure. Left panel: Evolution of integrase sequences obtained by quantitative deep sequencing. Neighbor Joining Tree with branch lengths computed according to a heterogeneous JTT + Γ model of protein evolution. This was the most likely tree to explain sequence evolution according to a Shimodaira–Hasegawa test (Shimodaira and Hasegawa, 1999). For clarity, monophyletic groups of sequences containing the same major integrase resistance mutation or combination of mutations were collapsed into a cartoon with colours indicating the explored mutation and the size of the cartoon being proportional to the number of sequences included. Right panels: Quartet likelihood mapping analysis of the origin of Q148R and N155H raltegravir-resistant viruses detected at virological failure. Four clusters of sequences containing, respectively, mutants at baseline (BL), mutants at virological failure (VF), wildtype (wt) viruses at BL; and wt viruses at VF were created. All possible quartets of sequences containing one sequence from each cluster were generated. A distance phylogenetic tree was then calculated for each sequence quartet and was compared with the phylogeny of each of our three hypotheses, shown in the triangle vertices. Numbers in the triangle show the proportion of quartet phylogenetic trees matching each hypothesis. The percentage of solved phylogenies is shown in the triangle vertices; unsolved phylogenies are represented in intermediate regions of the triangle. Separate analyses were performed for single Q148R (panel A) and single N155H (panel B) mutants at virological failure. Wildtype was defined as absence of major integrase inhibitor-resistant mutations at positions 143, 148 and 155.

method, we used the four-clustering likelihood mapping technique implemented in TREEPUZZLE v5.2 (Schmidt et al., 2002). In brief, we constructed 4 clusters of sequences containing, respectively, mutants detected at baseline, mutants present at virological failure, wildtype (wt) viruses found at baseline; and wt viruses observed at virological failure. Wildtype was defined as absence of major integrase inhibitor-resistant mutations at positions 143, 148 and 155. Then, we tested the hypotheses that mutant viruses at virological failure derived from baseline mutants, baseline wt, or wt at virological failure. These analyses were performed separately for Q148R and N155H mutants, excluding sequences with other major integrase resistance mutations than the one being tested (Table 2).

Genetic linkage between major and accessory mutations was investigated using in-house algorithms.

4. Results

Pre-treatment viruses were only susceptible to raltegravir and tenofovir (Fig. 1). Population sequencing detected the major raltegravir resistant mutations Q148R and N155H and the accessory G163R mutation at virological failure, mixed with the corresponding wild type. All other baseline mutations remained detectable at the time of virological failure.

Out of 3390 clonal sequences obtained with QDS before raltegravir initiation, nine (0.27%) had the Y143H/C mutation alone, four (0.12%) contained the Q148R mutation, one (0.03%) had the N155H mutation and none (0%) harbored two major mutations together. Of 3384 clonal sequences obtained with QDS at the time of virological failure, 1668 (49.29%) were single Q148R mutants, and 1575 (46.54%) had the N155H alone. Double Q148R + N155H mutants were found in 58 (1.71%) sequences at virological failure. Three baseline Q148R sequences were identical to 79/3384 (2.34%) sequences at virological failure, whereas the baseline N155H sequence was identical to 83/3384 (2.45%) sequences at virological failure.

The best evolutionary model obtained with PROTTESTv2.2 (HIVw + Γ with $\alpha = 2.921$) was used to perform the maximum likelihood tree; a Neighbor Joining distance tree was performed with the second best model detected by PROTTESTv2.2 (JTT + Γ with $\alpha = 3.204$), given that the best model is not implemented in MEGA4. A Shimodaira and Hasegawa test (Shimodaira and Hasegawa, 1999) considered the Neighbor Joining tree as the one most likely to explain the sequence evolution. The tree topology suggested that Q148R and the N155H mutants evolved in two separate clusters (Fig. 2). Most Q148R mutants found at VF originated from pre-existing Q148R mutants whereas N155H mutants found at VF could have originated from either the baseline N155H mutant or from baseline wildtype viruses. Double Q148R + N155H mutants were found interspersed at the edges of either Q148R or N155H cluster. Single Y143C/H mutants clustered together at baseline but were not

found at VF, suggesting that they were less fit, compared to Q148R and/or N155H, in the presence of raltegravir. A four-clustering likelihood mapping technique implemented in TREEPUZZLE v 5.2, independently supported the hypothesis that most Q148R and N155H mutants emerging at virological failure originated, respectively, from pre-existing Q148R and N155H mutants (Fig. 2).

No viruses with major raltegravir-resistant mutations had other mutations linked on the same genome before therapy initiation (not shown). Conversely, extensive associations between major and accessory mutations were observed at VF (Table 1). Only 6.5% and 7% of sequences, respectively, contained mutation Q148R and N155H alone at virological failure; all double Q148R + N155H mutants contained other accessory mutations.

5. Discussion

Our study shows that Q148R and N155H mutants developing during virological failure to raltegravir can originate from minority mutants generated spontaneously before treatment exposure. The spontaneous generation of mutants is predicted by extant models of viral replication in view of HIV-1's high turnover and the error-prone nature of its reverse transcriptase (Coffin, 1995; Najera et al., 1995). Here, mutants could not have been transmitted because integrase inhibitors had just been commercialized. The high antiviral potency of raltegravir (McColl and Chen, 2010) in a context of virtual dual therapy exerted potent selective pressure over pre-existing resistant viruses, as predicted from mathematical modeling of HIV resistance (Nowak et al., 1997).

Pre-existing mutants, however, were found below the error threshold of the technology; point errors at drug resistance sites converting a wildtype to a resistant mutation were 0.2% in our own controls and in previous studies (Shao et al., 2009; Wang et al., 2007). Nevertheless, two independent phylogenetic analyses indicated that pre-existing mutants were the most likely origin of Q148R and N155H mutants at virological failure; indeed, sequences identical to the baseline mutants were found in about 2% of viruses at virological failure. Using various technologies, other studies found pre-existing Q148R/H mutants at similar levels (Ceccherini-Silberstein et al., 2009; Charpentier et al., 2009).

Whereas baseline mutants did not incorporate other mutations in the genome region explored, more than 90% of viruses evolving during virological failure had accumulated accessory mutations in their genome. We cannot completely rule out that the presence of double Q148R + N155H mutants in 1.7% of viruses was due to PCR recombination (Shao et al., 2009), although it seems unlikely. The two mutations lie 6 codons apart and were found in similar proportions in two overlapping amplicons generated independently through separate triplicate PCRs. Interestingly, dual mutants often carried mutations E138K and G163R on the same genome. The ability of such accessory mutations to restore the impaired fitness of double Q148R + N155H mutants *in vivo* (Fransen et al., 2009) merits further investigation.

This case study provides further evidence that HIV-1 can escape from antiretroviral drug pressure through selection of pre-existing drug-resistant mutants. Our findings underscore the importance of prescribing fully active antiretroviral regimens to all HIV-1-infected subjects, as well as the need of developing more sensitive assays to detect transmitted as well as spontaneously generated drug-resistant minority variants.

Conflicts of interest

F. García has been a consultant on advisory boards, or has participated in speaker's bureaus, with Roche, Boehringer-Ingelheim, BMS, GSK, Gilead, Janssen, Merck and Pfizer. R. Delgado has received consulting fees and grant support from Abbott, BMS, Gilead and Roche. D. Dalmau has been a consultant on advisory boards, has participated in speaker's bureaus, or has conducted clinical trials with Roche, Boehringer-Ingelheim, Abbott, BMS, GSK, Gilead, Tibotec, Janssen, Merck and Pfizer. J. Martínez-Picado has received research funding, consultancy fees, or lecture sponsorships from GlaxoSmithKline, Merck and Roche. M. Álvarez-Tejado works for Roche Diagnostics S.L., Spain, which commercializes the 454 sequencing technology in Spain. B. Clotet has been a consultant on advisory boards, has participated in speakers' bureaus, or has conducted clinical trials with Roche, Boehringer-Ingelheim, Abbott, BMS, GSK, Gilead, Tibotec, Janssen, Merck, Pfizer, Siemens, Monogram Biosciences, and Panacos. R. Paredes has received consulting fees from Pfizer and grant support from Pfizer, Siemens, Merck and Boehringer Ingelheim. FM Codoñer, C. Pou, A. Thielen, MJ. Buzón, JR. Santos and L. Ruiz report no conflicts of interest relevant to this article. No other potential conflict of interest relevant to this article was reported.

Acknowledgements

This study was supported by the CDTI (Centro para el Desarrollo Tecnológico Industrial), Spanish Ministry of Science and Innovation (IDI-20080843); the Spanish AIDS network 'Red Temática Cooperativa de Investigación en SIDA' (RD06/0006), 'The European AIDS Treatment Network' (NEAT – European Commission FP6 Program, contract LSHP-CT-2006-037570) and 'CHAIN, Collaborative HIV and Anti-HIV Drug Resistance Network', Integrated Project no. 223131, funded by the European Commission Framework 7 Program. FMC was supported by the Marie Curie European Reintegration Grant number 238885, 'HIV Coevolution', also funded by the European Commission Framework 7 Program. This work was presented in part at the 8th European HIV Drug Resistance Workshop, 17–19 March 2010, Sorrento, Italy (Poster #51).

References

Abascal, F., Zardoya, R., Posada, D., 2005. ProtTest: selection of best-fit models of protein evolution. Bioinformatics 21, 2104–2105.

Buzon, M.J., Dalmau, J., Puertas, M.C., Puig, J., Clotet, B., Martinez-Picado, J., 2010. The HIV-1 integrase genotype strongly predicts raltegravir susceptibility but not viral fitness of primary virus isolates. Aids 24, 17–25.

Ceccherini-Silberstein, F., Armenia, D., D'Arrigo, R., Vandenbroucke, I., Van Baelen, K., Van Marck, H., Stuyver, L., Rizzardini, G., Antinori, A., Perno, C., 2009. Baseline variability of HIV-1 integrase in multi-experienced patients treated with raltegravir: a refined analysis by pyrosequencing. In: 16th Conference on Retroviruses and Opportunistic Infections, Montreal, Canada.

Charpentier, C., Piketty, C., Tisserand, P., Bélec, L., Laureillard, D., Karmochkine, M., Si-Mohamed, A., Weiss, L., 2009. Allele-specific real-time polymerase chain reaction of the presence of Q148H, Q148R, and N155H minority variants at baseline of a raltegravir-based regimen. In: 16th Conference on Retroviruses and Opportunistic Infections, Montreal, Canada.

Coffin, J.M., 1995. HIV population dynamics in vivo: implications for genetic variation, pathogenesis, and therapy. Science 267, 483–489.

Cooper, D.A., Steigbigel, R.T., Gatell, J.M., Rockstroh, J.K., Katlama, C., Yeni, P., Lazzarin, A., Clotet, B., Kumar, P.N., Eron, J.E., Schechter, M., Markowitz, M., Loutfy, M.R., Lennox, J.L., Zhao, J., Chen, J., Ryan, D.M., Rhodes, R.R., Killar, J.A., Gilde, L.R., Strohmaier, K.M., Meibohm, A.R., Miller, M.D., Hazuda, D.J., Nessly, M.L., DiNubile, M.J., Isaacs, R.D., Teppler, H., Nguyen, B.Y., 2008. Subgroup and resistance analyses of raltegravir for resistant HIV-1 infection. N. Engl. J. Med. 359, 355–365.

Edgar, R.C., 2004. MUSCLE: multiple sequence alignment with high accuracy and high throughput. Nucleic Acids Res. 32, 1792–1797.

Fransen, S., Gupta, S., Danovich, R., Hazuda, D., Miller, M., Witmer, M., Petropoulos, C.J., Huang, W., 2009. Loss of raltegravir susceptibility by human immunodeficiency virus type 1 is conferred via multiple nonoverlapping genetic pathways. J. Virol. 83, 11440–11446.

Guindon, S., Gascuel, O., 2003. A simple, fast, and accurate algorithm to estimate large phylogenies by maximum likelihood. Syst. Biol. 52, 696–704.

Kumar, S., Tamura, K., Nei, M., 2004. MEGA3: integrated software for molecular evolutionary genetics analysis and sequence alignment. Brief. Bioinform. 5, 150–163.

Liu, T.F., Shafer, R.W., 2006. Web resources for HIV type 1 genotypic-resistance test interpretation. Clin. Infect. Dis. 42, 1608–1618.

McColl, D.J., Chen, X., 2010. Strand transfer inhibitors of HIV-1 integrase: bringing in a new era of antiretroviral therapy. Antiviral Res. 85, 101–118.
Najera, I., Holguin, A., Quinones-Mateu, M.E., Munoz-Fernandez, M.A., Najera, R., Lopez-Galindez, C., Domingo, E., 1995. Pol gene quasispecies of human immunodeficiency virus: mutations associated with drug resistance in virus from patients undergoing no drug therapy. J. Virol. 69, 23–31.
Nowak, M.A., Bonhoeffer, S., Shaw, G.M., May, R.M., 1997. Anti-viral drug treatment: dynamics of resistance in free virus and infected cell populations. J. Theor. Biol. 184, 203–217.
Paredes, R., Clotet, B., 2010. Clinical management of HIV-1 resistance. Antiviral Res. 85, 245–265.
Rhee, S.Y., Gonzales, M.J., Kantor, R., Betts, B.J., Ravela, J., Shafer, R.W., 2003. Human immunodeficiency virus reverse transcriptase and protease sequence database. Nucleic Acids Res. 31, 298–303.
Schmidt, H.A., Strimmer, K., Vingron, M., von Haeseler, A., 2002. TREE-PUZZLE: maximum likelihood phylogenetic analysis using quartets and parallel computing. Bioinformatics 18, 502–504.
Shao, W., Boltz, V.F., Kearney, M., Maldarelli, F., Mellors, J.M., Stewart, C., Levitsky, A., Volfovsky, N., Stephens, R.M., Coffin, J.M., 2009. Characterization of HIV-1 sequence artifacts introduced by bulk PCR and detected by 454 sequencing. XVIII International HIV Drug Resistance Workshop: Basic Principles & Clinical Implications. Fort Myers, FL, USA, 9–13 June 2009 (Abstract 104). Antiviral Therapy 14 Suppl. 1, A123.
Shimodaira, H., Hasegawa, M., 1999. Multiple comparisons of log-likelihoods with applications to phylogenetic inference. Mol. Biol. Evol. 16, 1114–1116.
Steigbigel, R.T., Cooper, D.A., Kumar, P.N., Eron, J.E., Schechter, M., Markowitz, M., Loutfy, M.R., Lennox, J.L., Gatell, J.M., Rockstroh, J.K., Katlama, C., Yeni, P., Lazzarin, A., Clotet, B., Zhao, J., Chen, J., Ryan, D.M., Rhodes, R.R., Killar, J.A., Gilde, L.R., Strohmaier, K.M., Meibohm, A.R., Miller, M.D., Hazuda, D.J., Nessly, M.L., DiNubile, M.J., Isaacs, R.D., Nguyen, B.Y., Teppler, H., 2008. Raltegravir with optimized background therapy for resistant HIV-1 infection. N. Engl. J. Med. 359, 339–354.
Varghese, V., Shahriar, R., Rhee, S.Y., Liu, T., Simen, B.B., Egholm, M., Hanczaruk, B., Blake, L.A., Gharizadeh, B., Babrzadeh, F., Bachmann, M.H., Fessel, W.J., Shafer, R.W., 2009. Minority variants associated with transmitted and acquired HIV-1 nonnucleoside reverse transcriptase inhibitor resistance: implications for the use of second-generation nonnucleoside reverse transcriptase inhibitors. J. Acq. Immun. Def. Synd. 52, 309–315.
Wang, C., Mitsuya, Y., Gharizadeh, B., Ronaghi, M., Shafer, R.W., 2007. Characterization of mutation spectra with ultra-deep pyrosequencing: application to HIV-1 drug resistance. Genome Res. 17, 1195–1201.